Supplemental Material for: *Med12* Gain-of-Function Mutation Causes Leiomyomas and Genomic Instability

Authors: Priya Mittal[1], Yong-hyun Shin[2], Svetlana. A. Yatsenko[2, 3], Carlos.A.Castro[2], Urvashi Surti [1,2, 3], Aleksandar Rajkovic[1,2,3]

Affiliations:

[1]Department of Human Genetics, Graduate School of Public Health, University of Pittsburgh, Pittsburgh, PA,15261.

[2] Department of Obstetrics, Gynecology and Reproductive Sciences, Magee-Womens Research Institute, Pittsburgh, PA, 15213.

[3] Department of Pathology, University of Pittsburgh, Pittsburgh, PA, 15261.

Corresponding author: E-mail: rajkovica2@mail.magee.edu

Supplemental Methods

Generation of *Med12 Rosa* knock-in mice

Med12 Rosa knock-in mice were generated by introducing the most common missense mutation encountered in leiomyomas of American women, c.131G>A (p.Gly44Asp) (1), into the *Med12* cDNA. Full-length mouse *Med12* cDNA was cloned into pEntry vector (Invitrogen). The *Med12* 1.6 kbp fragment was PCR amplified from mouse newborn ovary cDNA, using the following primer set: pEntry-mMed12 F: CACCATGGCGGCTTTCGGGATCTT and pEntry-mMed12 R1: GCGGCCGCGAATTCTACTCGCTCACTT. The amplified *Med12* 1.6 kbp fragment was ligated with *Med12* EST clone (BC057119, GE Dharmacon) and EcoR1 and NOT1 cut 6.5 kbp fragment. The full-length *Med12* sequence (8.1 kbp) was confirmed by sequencing. Site-directed mutagenesis was performed using QuikChange Multi Site-Directed Mutagenesis Kit (Stratagene), with Mde12131AF:

ACGGCTTTGAATGTAAAACAAGATTTCAATAACCAGCCTGCTGTC and Mde12131AR:GACAGCAGGCTGGTTATTGAAATCTTGTTTTACATTCAAAGCCGT primers used according to manufacturer instructions. pROSA26-DV1 vector was used to target the *ROSA26* locus (2). Mutated *Med12* cDNA was inserted into the pROSA26-DV1, using LR Clonase Enzyme Mix (Invitrogen). Electroporation was performed, using G4 ES cells, at the MWRI transgenic core. Two ES cell clones were selected for blastocyst injection after confirming appropriate integration into the *ROSA 26* locus using *Rosa26* 5' probe (Rosa 5' probe F: GCTCAGAGACTCACGCAGCCCTAGT and rosa 5' probe R: AGAGTAGGGGGAGGGGAAGAGTCCT) and *Rosa26* 3' probe (Rosa 3' probe F:CTCCCAAGTGTTGGGAACTAAAGATA and *Rosa* 3' probe R: GCTACATCCTGATCTAGTCCTGAA) (Supplemental Figure2A,B). *Med12 R*OSA knock-in mice were maintained on a FVB/C57BL/6/129SV background.

Dr. Heinreich Schrewe generously donated the *Med12 flox* mice (3). The *Amhr2-Cre* mice were a kind gift of Dr. Richard Behringer (4). The *mT/mG* mice (GT(ROSA)26Sor$^{tm4(ACTB-tdTomato,-EGFP)Lou}$) were obtained from Jackson laboratory (Stock #007576). The DNA from tail biopsies was used to confirm the genotypes, using standard PCR protocols. The primer sets and the PCR protocol used to distinguish the *Med12*^{flox} wild-type and the recombined alleles in tissue genomic DNA have previously been described (3). The *Med12*^{flox} and *Amhr2-Cre* lines were maintained on a C57BL/6/129SV hybrid background. Litters were weaned at 3 weeks, and breeding pairs were set up at 6 weeks of age. All animals were housed under a 12-hour light, 12-hour dark schedule and provided food and water ad libitum.

Histology, immunohistochemistry, immunofluorescence, and Western blot analysis

Gross morphology and histology assessments were performed on adult female mice. Prior to harvesting the uteri, all females were estrous synchronized with IP injections of 5 IU PMSG followed by 5 IU of hCG after 48 hours. Females were euthanized 20 hours after hCG administration, and uteri were fixed in 10% formalin, processed, embedded in paraffin, serially sectioned (6 μm), and stained with hematoxylin and eosin. For Frozen sections, tissues were embedded in O.C.T. medium and were snap-frozen in liquid nitrogen. Sections were obtained using a Leica cryostat (6 μm). At least three pairs of uteri of each genotype were subjected to gross and microscopic analysis for each time point. Uteri were also subjected to Masson's Trichrome staining (American MasterTech). Images were acquired using an Axio Scope.A1 microscope (Zeiss) equipped with a digital camera (Zeiss) and an AxioVision (v4.8) imaging software.

Immunohistochemistry was performed on 6-μm paraffin sections and subjected to antigen retrieval using 10 mM sodium citrate (PH 6.0) for 20 min. For quenching endogenous peroxidase, sections were treated with 3% hydrogen peroxide and then blocked with 3% bovine serum albumin for 45 min, followed by incubation with anti-SMA (A5228, Sigma Aldrich) at 4°C overnight. Following primary antibody incubation, sections were washed and incubated in biotinylated secondary antibody for 30 min and ABC reagent (Vectastain). DAB Substrate Kit (Vector Labs) was then used to develop the immunoreactive signals.

Immunofluorescence was conducted on 6-μm frozen sections, using a similar protocol, except that the secondary antibodies were Alexa Fluor 488 (Life Technologies) and Alexa Fluor 647 (Life Technologies). Primary Anti-FLAG (F7425, Sigma Aldrich) antibody was used for immunofluorescence. The sections were mounted with Vectashield mounting medium containing DAPI. Images were taken with a Nikon A1 confocal microscope equipped with a digital camera and NIS-Elements software (Nikon).

To assess the fluorescent signals in the *mT/mG* reporter mice, frozen sections were washed three times in PBS and stained with DAPI. mT and mG signals were analyzed and scored in 300 uterine myometrial cells.

For Western blots, nuclear and cytoplasmic extracts were prepared from pulverized mouse uterine samples as described previously (5). Equal amounts of protein were loaded and resolved on 3-8% Tris-acetate gels (Life Technologies). Membranes were then incubated in either anti-FLAG (F7425, Sigma Aldrich) or β-tubulin antibodies (T0198, Sigma Aldrich) overnight at 4°C. The following day, the membranes were washed and incubated in respective secondary antibodies for 1 hour and developed using ECL-Prime (GE, Amersham).

DNA isolation

Genomic DNA was isolated from frozen tissue samples using DNeasy Blood & Tissue Kit (Qiagen) according to the manufacturer's protocol and was quantitated using a NanoDrop spectrophotometer (Thermo Scientific) as well as Qubit (Life Technologies).

Array CGH

Agilent SurePrint G3 Mouse Genome CGH 180K microarray kits were used to conduct array CGH on mouse uteri. Genomic DNA from uteri of four *Med12*$^{fl/+}$ *Med12R*$^{mt/+}$ *Amhr2-Cre* females was used as the "test" DNA and corresponding littermate control without *Amhr2-Cre* as the "reference" DNA. The samples were labeled, hybridized, and scanned according to the manufacturer's protocol. Briefly, 750 ng of test and reference DNA were digested with Alu I and Rsa I (Promega) and labeled with Cy3-dCTP (Test) or with Cy5- dCTP (Reference). The labeled DNA was purified and hybridized, washed, and scanned using an Agilent G2565CA Microarray Scanner. Raw data were obtained by Agilent Feature extraction software and imported into the Agilent Genomic Workbench 7.0 software for analysis. DNA copy number changes were detected by Genomic Workbench software. The ADM-2 statistical algorithm was used with a sensitivity of 6.0. The criteria for making aberration calls included positive calls by the software, $\log_2$ ratios of >0.25 or less than <-0.25, and the presence of three consecutive probes.

Human syntenic mapping

Mouse chromosomal aberrations were mapped onto human chromosomal loci using the UCSC genome browser LiftOver tool (http://genome.ucsc.edu). The gene lists for the

human intervals were determined by the microarray core website developed jointly by the University of Miami and Oklahoma University (www.ccs.miami.edu/cgi-bin/ROH/ROH_analysis_tool.cgi).

Reverse transcription, quantitative real-time PCR, and *Med12* variant expression detection

Total RNA was isolated from frozen uteri using the RNeasy Mini Kit (Qiagen). One microgram of total RNA was reverse transcribed using Superscript III reverse transcriptase (Invitrogen). *Med12* gene expression was analyzed by real-time quantitative polymerase chain reaction. A SYBR Green detection system (Bio-Rad CFX96 PCR Detect System) was used, along with customized *Med12* primer sets: Med126-7F: CTGACTTGGGTGCTTGAGTGTT and Med126-7R: CCAATCTCCGGGTACAGAAGTA. Melt curve analysis was performed when using SYBR Green to verify a single amplification peak. Data were normalized to an endogenous reference (*GAPDH*) and then relative mRNA expression was calculated using the $2^{-\Delta\Delta C}$ method.

Med12 exon 2 C.131 G>A variant was detected in mutant mouse uteri by performing PCR, followed by Sanger sequencing using the following forward and reverse oligonucleotide that bracketed the *Med12* exon 2 C.131 G>A variant: *Med12* F: ATGGCGGCTTTCGGGATCTT and *Med12* R: AGTTGGAACTGATCTTGGCAGG primers, designed in Primer3 (http://bioinfo.ut.ee/primer3-0.4.0). Sequencing results were analyzed using Sequencher software.

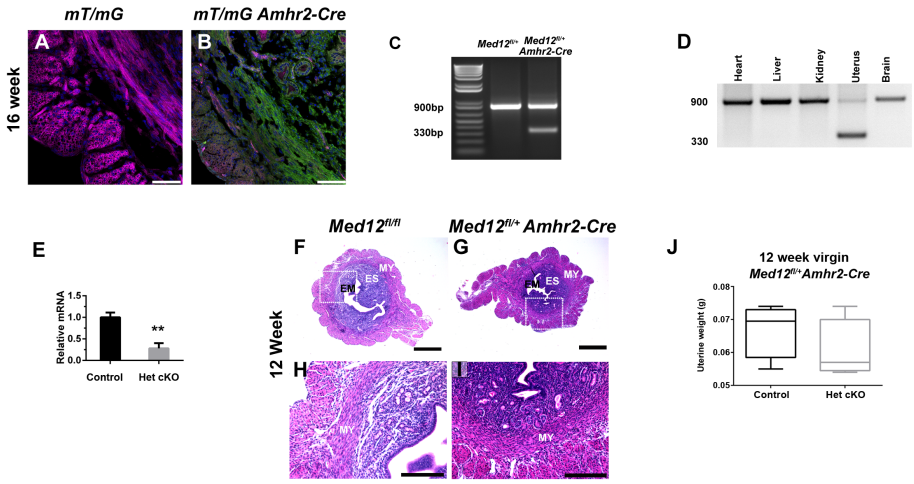

Supplemental Figure 1. Evaluation of *Amhr2-Cre* activity and histology of uteri with loss of *Med12*. We used *mT/mG* mice to assess the efficiency of *Amhr2-Cre* recombination. **(A)** 16-week-old *mT/mG* mice display ubiquitous mT (Tomato) labelling prior to recombination. **(B)** 16-week-old *mT/mGAmhr2-Cre* uteri display mG (Green) expression in cells having undergone cre-mediated excision. The non-recombined cells still display mT expression. **(C)** Recombination of *Med12* floxed alleles in uterine genomic DNA of *Med12*$^{fl/+}$ *Amhr2-Cre* females. *Med12* recombined bands are detected at 330 bp in the genomic DNA of cKO but not in the uterine genomic DNA of controls (*Med12*$^{fl/fl}$). **(D)**The recombined bands (330 bp) were only detected in the genomic DNA of the uterus and not in other tissues such as the liver, heart, or kidneys. **(E)** Relative *Med12* mRNA levels are down-regulated in uteri of *Med12* cKO (n=4) as compared to *Med12*$^{fl/fl}$ uteri (n=4). Relative mRNA levels of *Med12* were normalized to *Gapdh.* The mRNA expression studies were replicated on n=4 samples three independent times. Histological evaluation of 12 week old nulliparous **(F)** control, *Med12*$^{fl/fl}$, uteri and **(G)** loss of function, *Med12*$^{fl/+}$ *Amhr2-Cre*, uteri reveals no differences in histology

and lack of leiomyoma-like lesions. We have also analyzed the uterine histology of 4-month-, 6-month-, and 8-month-old *Med12*$^{fl/+}$ *Amhr2-Cre* females (n=10) and have not observed uterine tumors. The white dotted regions in panels **(F)** and **(G)** are shown at higher magnification in panels **(H)** and **(I),** respectively. **(J)** Uterine weights of *Med12*$^{fl/+}$ *Amhr2-Cre* mice (n=7) did not significantly differ from that of *Med12*$^{fl/+}$, $p>0.05$. Data are presented as mean ± SD. ES-endometrial stroma; MY-myometrium; EM-endometrium. Scale Bars = 0.2μm **(F,G)**, 20μm **(H,I).**

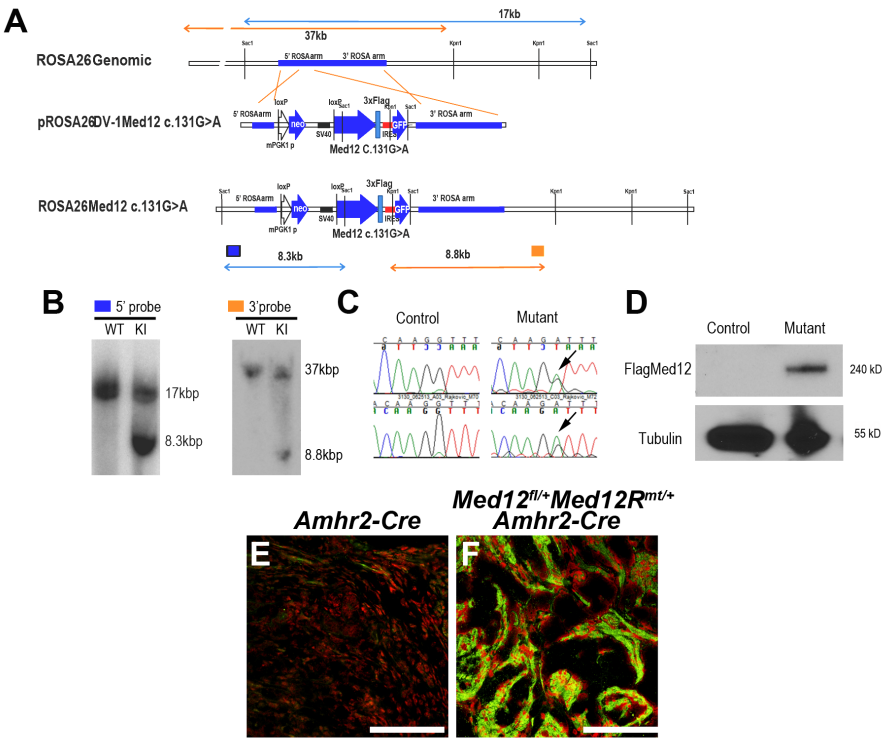

Supplemental Figure 2. Generation of *ROSA26 Med12 c.131G>A* mice that conditionally express *Med12 c.131G>A* variant. (A) Mouse *Med12* cDNA was mutated and inserted into the pROSA26-DV1 vector (pROSA26DV-1Med12 c.131G>A) and electroporated into G4 ES cells for homologous recombination with *ROSA26* genomic locus to generate *ROSA26 Med12* c.131G>A mice.

Mutated *Med12* transcripts expressed from the *ROSA26* locus are fused with FLAG and GFP. (**B)** Southern blot on DNA extracted from recombined G4 ES cells shows targeting of mutated *Med12* to the *ROSA26* locus. Probes corresponding to the 5' (blue) and 3' (orange) targeting ends are expected to generate 17-Kb wild-type and 8.4-kb mutant fragments and 37-kb wild-type and 8.8-kb mutant fragments, respectively, when genomic DNA is digested with Sac I and Kpn I enzymes. **(C)** Uteri from mice that carry the mutation in the absence of *Amhr2-Cre* (*Med12*$^{fl/+}$ *Med12R*$^{mt/+}$) do not express mutant mRNA, while in the presence of *Amhr2-Cre* (*Med12*$^{fl/+}$ *Med12R*$^{mt/+}$ *Amhr2-Cre*), uteri show significant expression of mutant c.131G>A variant (green chromatogram peak, black arrows). **(D)** Western blot analysis shows expression of mutant Med12 protein fused with FLAG in *Med12R*$^{mt/+}$ *Amhr2-Cre* uteri as compared to control (*Med12R*$^{mt/+}$) uteri that are devoid of *Amhr2-Cre*. Tubulin is used as a loading control. **(E,F)** Immunostaining with FLAG antibody shows FLAG expression as a marker for mutant Med12 expression in uteri of *Med12*$^{fl/+}$ *Med12R*$^{mt/+}$ *Amhr2-Cre* females as compared to control uteri (*Amhr2-Cre*). These results indicate that tumors express mutant *Med12*. Green: FLAG expression, Red: DAPI staining. Scale bars = 50μm (E,F).

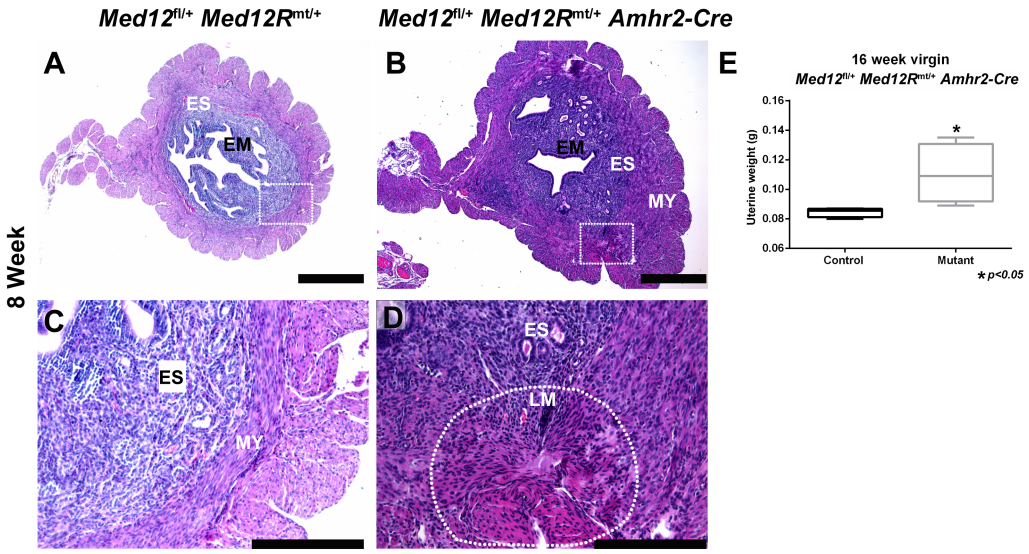

Supplemental Figure 3. Histological evaluation of uteri from *Med12$^{fl/+}$ Med12R$^{mt/+}$ Amhr2-Cre* females. (A) Control animals (*Med12$^{fl/+}$ Med12R$^{mt/+}$*) show normal uterine histology; a magnified view of the white box shows normal endometrial stroma (ES) and myometrium (MY) in **(C). (B)** Pathological changes associated with leiomyomas, including hyperplasia, are observed as early as 8 weeks (three of four females) in uteri expressing *Med12 c.131G>A* variant on the background of conditional *Med12* loss (*Med12$^{fl/+}$ Med12R$^{mt/+}$ Amhr2-Cre)*. A higher magnification of the white outlined box appears in **(D)**, which shows leiomyoma-like lesions characterized by extracellular matrix deposits and dispersed nuclei. **(E)** Mutant uteri weights (n=4) at 16 weeks were significantly higher than controls (n=4) (p<0.05). Uterine weights were determined from four animals in each group. Data are presented as mean ± SD. LM-leiomyoma; ES-endometrial stroma; MY-myometrium; EM-endometrium. Scale Bars = 0.2μm (A,B), 20μm (C,D).

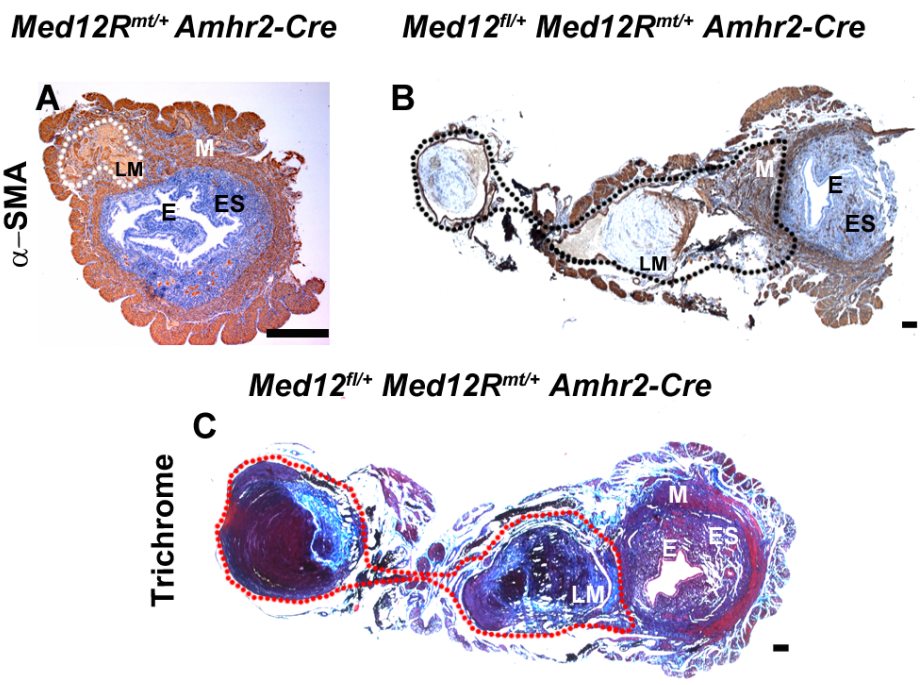

Supplemental Figure 4. Molecular characterization of leiomyoma-like lesions in mutant *Med12* uteri. (A) and **(B)** are representative images from *Med12R*$^{mt/+}$ *Amhr2-Cre* and *Med12*$^{fl/+}$ *Med12R*$^{mt/+}$ *Amhr2-Cre* mice, showing immunoreactivity to anti-SMA antibodies and staining with Masson's Trichrome. Anti-SMA antibodies show immunoreactivity (brown) in the leiomyoma-like lesion (LM) outlined with a dotted white line. SMA is a marker for smooth muscle cells. Collagen deposits within the uterine tumors stain blue with Masson's Trichrome **(C)**. Red stains show muscle fibers; the blue stain indicates an abundance of collagen deposition in the tumor lesion, a known characteristic of leiomyomas. ES- endometrial stroma; M- myometrium; E- endometrium Bars = 0.2μm (A), 100μm (B, C).

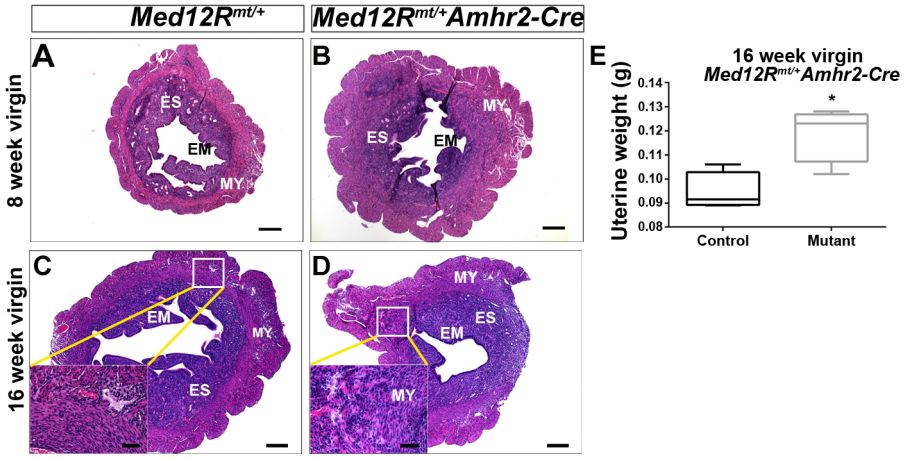

Supplemental Figure 5. Histological evaluation of uteri from *Med12R*$^{mt/+}$ *Amhr2-Cre* females. (A,B) No significant pathological changes other than hyperplasia are observed in uteri of *Med12R*$^{mt/+}$ *Amhr2-Cre* at 8 weeks of age (three out of four mice), as shown in **(B)** as compared to controls (*Med12R*$^{mt/+}$) in **(A). (C,D)** No abnormal lesions were observed in uteri of control mice **(C)**, while four out of eight uteri from 12-week-and-older *Med12R*$^{mt/+}$ *Amhr2-Cre* females **(D)** showed leiomyoma-like lesions displaying disorganized muscle fiber arrangement and extracellular matrix deposition associated with leiomyoma formation. Insets in **(C)** and **(D)** are amplified regions in white squares. **(E)** Uteri of *Med12R*$^{mt/+}$ *Amhr2-Cre* females (n=4) weighed significantly higher than those of control (*Med12R*$^{mt/+}$) females (n=4). Data are presented as mean ± SD. LM-leiomyoma; ES-endometrial stroma; MY-myometrium; EM-endometrium. Scale Bars = 200μm (A,B,C,D), 50 μm (insets).

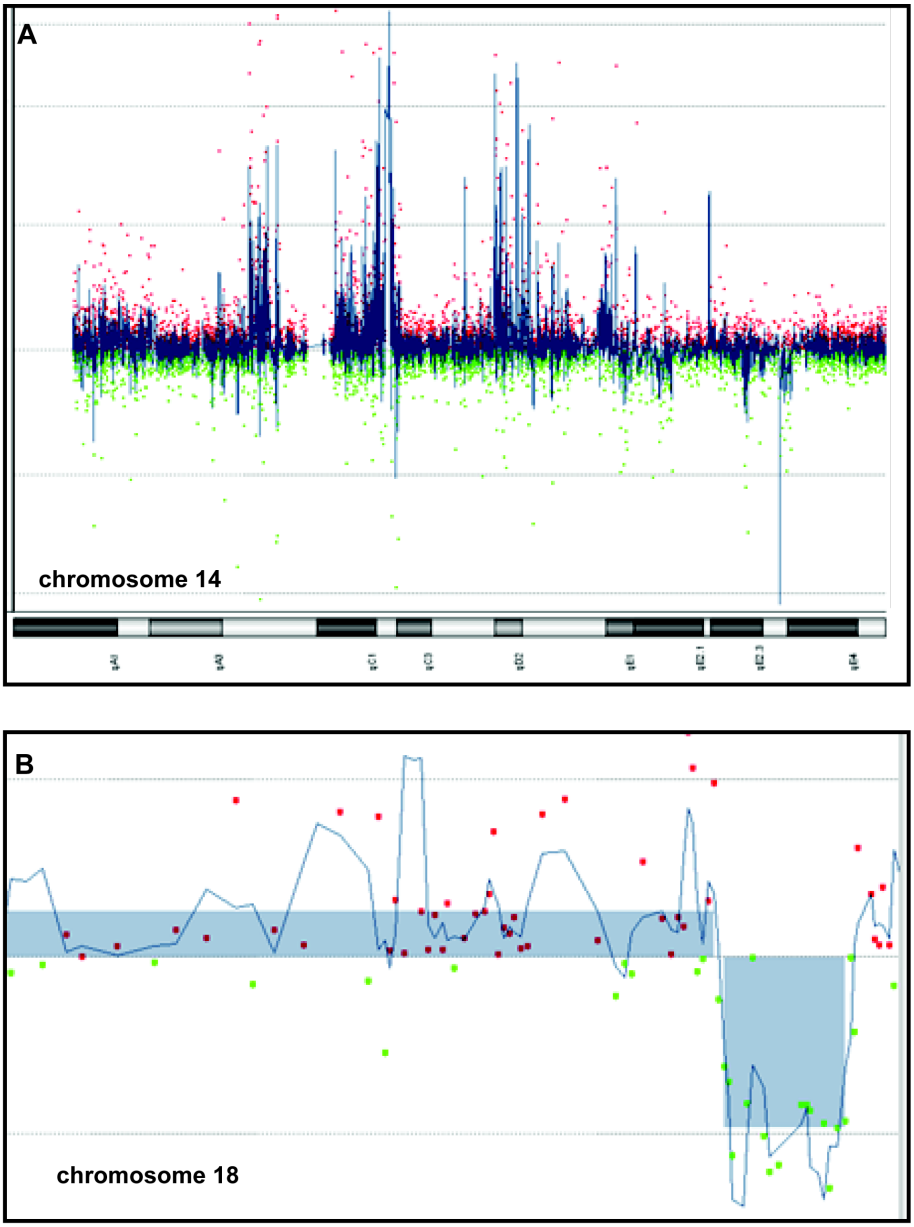

Supplemental Figure 6. **Representative array profiles from tumors of *Med12*$^{fl/+}$ *Med12R*$^{mt/+}$ *Amhr2-Cre* females. (A)** Chromosome view of mouse chromosome 14 of *Med12*$^{fl/+}$ *Med12R*$^{mt/+}$ *Amhr2-Cre* uteri showing chromothripsis. **(B)** Representative example of mosaic gain followed by a loss of region 18qA1 (chr18: 8457226-10017847). This region of approximately 345 kb encompasses the genes *Fzd8, Ccny, Cetn1, Thoc1, Usp14*, and *Colec12*.

Chromosome	Cytoband	Start	Stop	Aberration size (Kb)	Gain/Loss	Region of Aberration
chr1	qD	90115633	90193738	78.105	deletion	3
chr1	qE1.1	101591968	101656500	64.532	gain	1
chr1	qH4	179805696	179926632	120.936	deletion	1
chr1	qH5	187079059	187183640	104.581	gain	1
chr2	qA1	3947206	4016684	69.478	deletion	3
chr2	qC1.3	62554677	62580394	25.717	deletion	4
chr2	qD	85849412	85920056	70.644	gain	4
chr2	qH2	161545931	161698753	152.822	gain	1
chr3	qF1	87188304	87211687	23.383	gain	1
chr3	qF1	87267733	87302881	35.148	gain	1
chr3	qF3	110878881	110995945	117.064	gain	1
chr4	qD1	111726014	113251939	1525.925	deletion	4
chr4	qD1	111742887	112273763	530.876	deletion	4
chr4	qD1	111962345	112065411	103.066	deletion	4
chr4	qD1	112289418	112504314	214.896	deletion	3
chr4	qD1	112510205	112564300	54.095	deletion	4
chr4	qD1	112665000	112793116	128.116	deletion	4
chr4	qD1	112821289	112915923	94.634	deletion	4
chr4	qD1	113001582	113251939	250.357	deletion	2
chr4	qD1	113286238	113658273	372.035	deletion	1
chr4	qD2.2	121649423	122218644	569.221	deletion	1
chr4	qD2.3	132799884	132936192	136.308	deletion	1
chr4	qE1	145001092	146793868	1792.776	deletion	3
chr5	qC3.1	69891606	70097860	206.254	gain	3
chr5	qE5	105142362	105237345	94.983	gain	1
chr6	qA1	8556759	8575270	18.511	gain	1
chr6	qB1	41010073	41112757	102.684	gain	1
chr6	qB1	41306470	41412425	105.955	gain	2
chr7	qA2	18382929	18426616	43.687	gain	1
chr7	qB4	54844755	54883844	39.089	deletion	2
chr7	qB4	55466579	55715246	248.667	gain	1
chr7	qC	67475144	67731725	256.581	deletion	1
chr7	qE3	111430424	111507023	76.599	deletion	1
chr7	qF1	123631491	123927328	295.837	deletion	2
chr7	qF3	136825759	137141925	316.166	gain	1
chr8	qA1.2	16763830	16826155	62.325	gain	1
chr8	qA4	40187843	40274870	87.027	gain	1
chr9	qA3	21968269	22021024	52.755	deletion	1
chr9	qA5.3	46697499	46906183	208.684	deletion	0
chr10	qA3	17697339	17744401	47.062	deletion	1
chr10	qA3	22006887	22072759	65.872	gain	1

chr12	qE	105048428	105263855	215.427	deletion	2
chr12	qF1	114886825	114956321	69.496	gain	4
chr12	qF1 - qF2	115427710	115487987	60.277	deletion	4
chr12	qF2	115667710	115852666	184.956	gain	4
chr12	qF2	116155408	116261498	106.09	deletion	4
chr12	qF2	116515691	116624944	109.253	deletion	4
chr12	qF2	116840011	117047397	207.386	gain	
chr12	qF2	117198164	117274793	76.629	deletion	
chr13	qA1	12690823	12723384	32.561	Deletion	2
chr13	qB3	61743712	62048006	304.294	gain	1
chr13	qC1	75983645	76020728	37.083	Deletion	1
chr13	qD1	101053361	101110842	57.481	deletion	1
chr14	qC1	44380406	44579789	199.383	Gain	1
chr14	qC2	54320774	54422503	101.729	gain	1
chr14	qD1	69019011	69103662	84.651	gain	1
chr14	qD2	69209459	69249991	40.532	gain	1
chr14	qD2	69876584	70090608	214.024	deletion	2
chr14	qD2	72891034	72930683	39.649	gain	1
chr14	qD3	84908855	85042415	133.56	gain	1
chr14	qE1	86407031	86441138	34.107	gain	1
chr14	qE3	110472070	111123931	651.861	deletion	1
chr14	qE3 - qE4	110015732	111565569	1549.837	deletion	1
chr15	qA1	14992022	15100240	108.218	gain	
chr15	qE1	77310653	77364452	53.799	gain	3
chr16	qB3	35483725	35550180	66.455	gain	1
chr16	qB3	36245661	36336077	90.416	deletion	1
chr16	qB4	44819587	44909082	89.495	gain	1
chr17	qA3.3	30586287	31049473	463.186	gain	4
chr17	qB1	36199712	36245963	46.251	gain	1
chr17	qB1	36860348	36909276	48.928	deletion	1
chr17	qB1	38635045	38791870	156.825	gain	1
chr17	qB1 - qB2	40082709	40241053	158.344	deletion	4
chr18	qA1	8457226	9788370	1331.144	gain	1
chr18	qA1	9813671	10017847	204.176	deletion	3
chr19	qD3	60897053	60945155	48.102	Gain	1

Table S1: Chromosomal aberration list of all four mouse tumors, with the respective intervals

Mouse	Human	Human		Orthologous genes			
Chromosome	chromosomal locus	Start	Stop	Tumor 1	Tumor 2	Tumor 3	Tumor 4
4qD2.3	chr1	27470631	27690372			SLC9A1,CHCHD3P3,WDTC1,SYTL1,MAP3K6	
3qF3	chr1	106701046	106830733	-	-		
3qF1	chr1	157764252	157772664			FCRL1	
1qH5	chr1	220229780	220359711	BPNT1,IARS2,MIR215,MIR194-1,RAB3GAP2			
13qA1	chr1	236368354	236390748			ERO1LB,GPR137B	ERO1LB,GPR137B
1qH4	chr1	244734347	244817416		DESI2,COX20		
1qE1.1	chr2	124573472	124762072				
2qC1.3	chr2	163236878	163260207				
1qD	chr2	234682002	234812683		HJURP,TRPM8,SPP2	HJURP,MSL3P1	HJURP,MSL3P1,TRPM8
16qB3	chr3	122738925	122793361			SEMA5B,PDIA5	
5qC3.1	chr4	44613169	44931460		GNPDA2	YIPF7,GUF1,GNPDA2	YIPF7,GUF1,GNPDA2
8qA4	chr4	190221667	190228149				
13qC1	chr5	95111576	95153221			RHOBTB3,GLRX	
15qA1	chr5	29027869	29199306				
13qD2.3	chr5	45614983	45626841	HCN1	HCN1		
13qD1	chr5	66052023	66071066				
13qD1	chr5	70265907	70308766		NAIP		
17qA3.3	chr6	38457579	39028735	BTBD9,GLO1,DNAH8,GLP1R	BTBD9,GLO1,DNAH8,GLP1R	BTBD9,GLO1,DNAH8	BTBD9,GLO1,DNAH8,GLP1R
10qA3	chr6	139348580	139403048			ABRACL	ABRACL
6qA1	chr7	8134096	8148036				
6qB1	chr7	142190236	142250584				
8qA4	chr8	15586895	15636766		TUSC3		
14qD2	chr8	23158977	23414178		LOXL2,ENTPD4,SLC25A37		
14qD2	chr8	24187964	24229697	ADAM28			

14qD1	chr8	24383271	24461193				
14qD2	chr8	36716399	36733668	KCNU1			
8qA1.2	chr8	3989107	4060094				
2qA1	chr10	14283901	14363312			FRMD4A	FRMD4A
18qA1	chr10	35739803	36669673	CCNY,GJD 4,FZD8			
19qD3	chr10	120876971	120932106				SFXN4, COXPD13, PRDX3
7qF3	chr10	122740826	123058528				
2qD	chr11	56216083	56241010		SLC25A37		
9qA5.3	chr11	115811243	116008575	KCNU1			
14qD3	chr13	58275467	58409706	PCDH17			
14qE1	chr13	59632641	59660044				
14qE3 - 14qE4	chr13	85181293	87535910			SLITRK6, MOB1AP1, DDX6P2, TXNL1P1	
14qE3	chr13	85660155	86345915				
12qE	chr14	94879399	94946027			SERPINA11, SERPINA9	
12qF1	chr14	106209967	106242264				
7qF1	chr16	18175137	18325190				
11qB5	chr17	2938562	2948297				
11qB4	chr17	5417772	5463831		NLRP1		
18qA1	chr18	179212	391932	USP14,TH OC1,COLE C12	USP14,TH OC1,COLE C12		USP14,THOC1,C OLEC12
2qH2	chr20	40900568	41046759				PTPRT

Table S2: List of human chromosomal intervals that are syntenic to mouse chromosomal aberration intervals and conserved orthologous genes in the conserved regions

References

1. McGuire MM, Yatsenko A, Hoffner L, Jones M, Surti U, and Rajkovic A. Whole exome sequencing in a random sample of North American women with leiomyomas identifies MED12 mutations in majority of uterine leiomyomas. *PloS one.* 2012;7(3):e33251.
2. Nyabi O, Naessens M, Haigh K, Gembarska A, Goossens S, Maetens M, De Clercq S, Drogat B, Haenebalcke L, Bartunkova S, et al. Efficient mouse transgenesis using Gateway-compatible ROSA26 locus targeting vectors and F1 hybrid ES cells. *Nucleic Acids Research.* 2009;37(7).
3. Rocha PP, Scholze M, Bleiss W, and Schrewe H. Med12 is essential for early mouse development and for canonical Wnt and Wnt/PCP signaling. *Development.* 2010;137(16):2723-31.
4. Jamin SP, Arango NA, Mishina Y, Hanks MC, and Behringer RR. Requirement of Bmpr1a for Mullerian duct regression during male sexual development. *Nature genetics.* 2002;32(3):408-10.
5. Jeyasuria P, Wetzel J, Bradley M, Subedi K, and Condon JC. Progesterone-regulated caspase 3 action in the mouse may play a role in uterine quiescence during pregnancy through fragmentation of uterine myocyte contractile proteins. *Biology of reproduction.* 2009;80(5):928-34.